



HAL
open science

Civil Aviation GALILEO E5 receivers architecture

Frédéric Bastide, Benoit Roturier, Olivier Julien, Christophe Macabiau, Emilie Rebeyrol, Mathieu Raimondi, Christophe Ouzeau, Damien Kubrak

► **To cite this version:**

Frédéric Bastide, Benoit Roturier, Olivier Julien, Christophe Macabiau, Emilie Rebeyrol, et al.. Civil Aviation GALILEO E5 receivers architecture. CNES-ESA, 1st Workshop on GALILEO Signals and Signal Processing, Oct 2006, Toulouse, France. hal-01021797

HAL Id: hal-01021797

<https://enac.hal.science/hal-01021797v1>

Submitted on 27 Oct 2014

HAL is a multi-disciplinary open access archive for the deposit and dissemination of scientific research documents, whether they are published or not. The documents may come from teaching and research institutions in France or abroad, or from public or private research centers.

L'archive ouverte pluridisciplinaire **HAL**, est destinée au dépôt et à la diffusion de documents scientifiques de niveau recherche, publiés ou non, émanant des établissements d'enseignement et de recherche français ou étrangers, des laboratoires publics ou privés.

Civil Aviation Galileo E5 Receivers Architecture

Frédéric Bastide, Benoît Roturier, DTI

O.Julien, C.Macabiau, E.Rebeyrol, M.Raimondi,
C.Ouzeau, D.Kubrak, ENAC

1 Introduction

The Galileo E5 signal is of particular interest to the civil aviation community. Indeed, it will be broadcast in an Aeronautical Radio Navigation Services (ARNS). Moreover, combined with the Galileo E1 signal, Galileo E5 will allow dual-frequency ionospheric-free pseudorange combinations supporting a dramatic increase of accuracy. In addition, one of its components, E5b, will carry the Galileo integrity message needed by the user to benefit from the Safety-of-Life service (SoL).

Civil aviation users have specific requirements in terms of performance of future Galileo receivers. Those requirements are provided by EUROCAE in the interim Minimum Operational Performance Specification (MOPS) document as developed by the Working Group 62. One important minimum requirement is for the receiver to process independently Galileo E5a and E5b signals mainly in order to reduce interference impact and to benefit from the Safety-of-Life (SoL) service. There are different possible signal processing techniques to build a civil aviation receiver achieving the performance requirements which are stated in terms of accuracy and robustness to interference, for instance.

This paper presents an overview of the different signal processing techniques expected to be implemented in future Galileo E5 receivers to meet civil aviation requirements. Most of the presented techniques were considered by EUROCAE WG62 to derive requirements. Some new techniques which could provide increased performance, at the cost of an increased complexity in general, are presented as well. The levels of performance achieved by all those techniques are indicated.

In the first section of this paper, the Galileo E5 signal, as described in the Galileo SIS ICD, is shortly presented. Then, the architecture of the receiver is described along with the main functions involved and their respective performance for Galileo E5 signal. These functions are: RF/IF filtering, the blanker system (temporal and frequency-based: FDAF), the acquisition process (temporal and frequency-based), tracking process and interference detection techniques.

2 Galileo E5 Signal

The Galileo E5 signal consists of four components which transmit two categories of services: the Open Service (OS) on the E5a band, divided into a data and a pilot channels, and the Safety of Life (SoL) service on the E5b band, also divided into a data and a pilot channel. These four components have the following characteristics [GalICD]:

- For the E5a data channel: it results from the modulation of the E5a navigation data stream with the E5a data channel PRN tiered code sequence which has a 10.23 Mcps chipping rate.
- For the E5a pilot (dataless) channel: it consists in the E5a pilot channel PRN tiered code sequence which has a 10.23 Mcps chipping rate.
- For the E5b data channel: it results from the modulation of the E5b navigation data stream with the E5b data channel PRN tiered code sequence which has a 10.23 Mcps chipping rate. The E5b navigation data stream contains integrity messages needed to be compliant with the civil aviation requirements (SoL service).
- For the E5b pilot channel: it consists in the E5b pilot channel PRN tiered code sequence which has a 10.23 Mcps chipping rate.

At the E5 band, the modulation choice is to multiplex, on a same carrier, two different QPSK-like services while keeping the properties of an Offset Carrier signal (with split spectrum properties defining a lower E5a band and an upper E5b band) and a constant envelope. This modulation is called constant envelope Alternate Binary Offset Carrier (ALTBOC) modulation. It is proposed with a code chipping rate of 10.23 Mcps and sub-carriers of 15.345 MHz, leading to an ALTBOC(15,10) configuration. The expression of the constant envelope ALTBOC modulation power spectrum density is equal to the following equation and is represented in Figure 1 (E5a and E5b main lobes are indicated in this figure), [Rebeyrol et al., 2005].

$$G_{ALTBOC}(f) = \frac{4}{\pi^2 f^2 T_c} \frac{\cos^2(\pi f T_c)}{\cos^2\left(\pi f \frac{T_c}{n}\right)} \left[\cos^2\left(\pi f \frac{T_s}{2}\right) - \cos\left(\pi f \frac{T_s}{2}\right) - 2 \cos\left(\pi f \frac{T_s}{2}\right) \cos\left(\pi f \frac{T_s}{4}\right) + 2 \right]$$

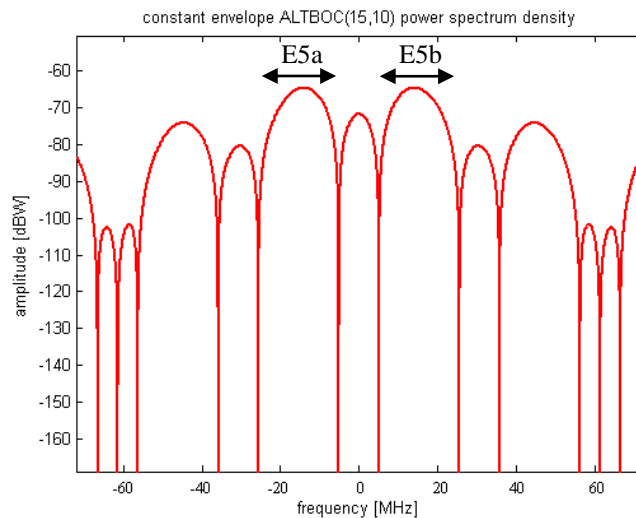


Figure 1

Figure 1 - Constant Envelope ALTBOC(15,10) Normalized Power Spectrum Density

The split spectrum characteristic of the E5 AltBOC modulation was considered by the EUROCAE WG62 to enable the separate processing Galileo E5a and E5b signals that can be viewed as QPSK signals.

3 Receiver Architecture

The block diagram of a generic GNSS receiver is depicted in Figure 2.

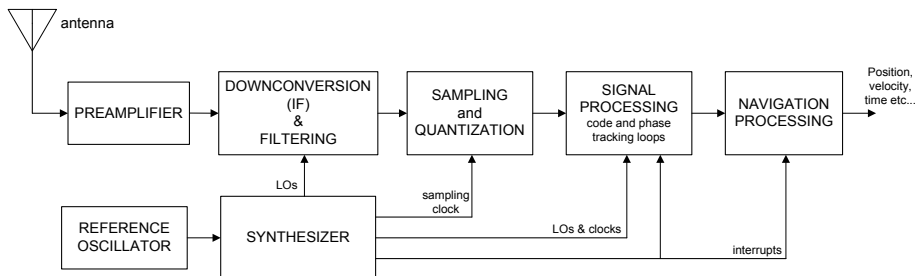


Figure 2 - GNSS Receiver Block Diagram

Different functions of this receiver will be specific for the Galileo E5 signal. The most significant ones are analyzed in the following.

3.1 RF/IF Filtering

The current baseline in the interim Galileo receivers MOPS [GalMOPS] is to isolate as much as possible, at the front-end level, E5a and E5b signals. The objectives are to reduce the risk of common interference and to process them independently on different receiver channels. Moreover, only Galileo E5b is required to benefit from the SoL service. Note this is a minimum requirement meaning a receiver manufacturer may decide to make receivers processing, additionally, Galileo E5 coherently as a single wideband signal. The EUROCAE MOPS defines minimum RF/IF filtering requirements on E5a and E5b which are depicted in Figure 3.

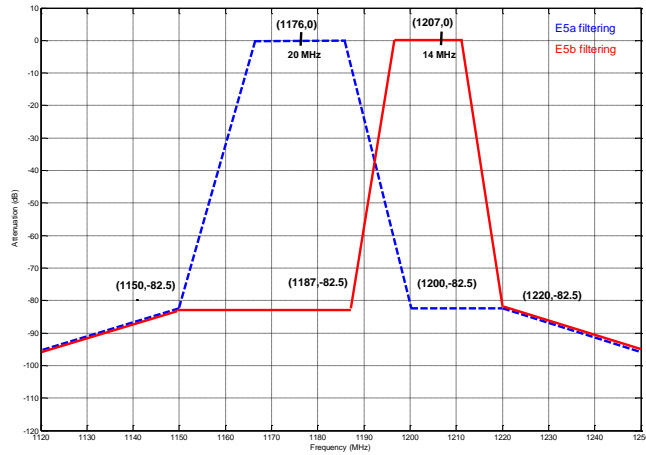


Figure 3

Figure 3 - Galileo MOPS Filtering Requirements on E5a and E5b Bands

On E5a, the passband is [E5a-10 MHz,E5a+10 MHz] while on E5b it is [E5b-10 MHz,E5b+4 MHz]. This latter passband is reduced towards upper frequencies to minimize the impact of *Out-of-Band* emissions from radars operating in the 1215-1385 MHz range.

3.2 Blanking System

The expected E5 band interference environment is presented in the EUROCAE Galileo MOPS [GalMOPS] as well as in [RTCA DO-292] for the L5/E5a band. It is documented that systems of significant infrastructure already exist in the E5 frequency band, with the main threat being the pulsed DME/TACAN signals. The initial proposal on how to cope with these signals was to implement a pulse detection and blanking circuitry. This circuitry consists in mitigating the parts of the incoming signal which contain high-level interference pulses. There are different possible implementations of the blanker. Two potential implementations for civil aviation receivers are presented in section 3.2.1 and 3.2.2. The first one is a blanker working on temporal samples while the second one relies on frequency-domain samples.

3.2.1 Temporal Blanker

The blanking circuitry was first proposed using a temporal analog technology as explained in [Hegarty] but a temporal digital solution was later proposed [Grabowsy]. This latter method is much simpler because no pulse detector circuit is required to identify the beginning and the end of each pulse. Furthermore, the implementation does not need memory to track samples that are part of a pulse. The quantized samples at the Analog to Digital Converter (ADC) output are zeroed on a sample-by-sample basis when their amplitude, or power, is above a predetermined blanking threshold, that can be based on the expected incoming samples noise level. EUROCAE WG62 considered this blanking technique to assess the Galileo receiver susceptibilities to DME/TACAN and JTIDS/MIDS pulsed interference [Appendix D of the MOPS]. Over the European hot-spot (50°N, 9° East, altitude of 40.000 feet), considered as the most critical aircraft location with respect to pulsed interference threat, the estimated equivalent C/N_0 degradations for Galileo E5a et E5b signals due to DME/TACAN and JTIDS/MIDS pulsed interference are summarized in Table 1 for blanking thresholds equal to -117.1 dBW and -120.0 dBW respectively [Bastide1].

Maximum C/N_0 degradation (dB)/ @ FL 400	Europe	
	Galileo E5a Th=-117.1 dBW	Galileo E5b Th=-120.0 dBW
JTIDS/MIDS case VIII only	1.9	1.2
DME/TACAN only	8.1	6.4
DME/TACAN+JTIDS/MIDS case VIII	8.9	7.3

Table 1 - Maximum C/N_0 degradation over the European hot-spots for Galileo E5a a and E5b

The level of degradation observed in Table 1 (representing the worst case scenario) complies with the EUROCAE requirements for acquisition and tracking minimum C/N_0 values. Thus, even if the equivalent C/N_0

degradation can be important, this method is likely to be the one selected in future GNSS receivers as a result of the simplicity of the design.

3.2.2 Frequency-Domain Blanker

The Frequency Domain Adaptive Filtering (FDAF) technique is a pulsed interference removal technique working in the frequency domain. The idea behind the FDAF technique is to limit the main limitation of pulse blanking which is the partial blanking of the DME/TACAN pulses. Indeed, due to the carrier modulating the pulse, many samples are below the temporal blanking threshold. By removing the frequency component associated with the pulse, this temporal limitation should be removed. The relative narrow frequency span of DME/TACAN signals (~1 MHz) as compared to the Galileo E5a/E5b signals (~20 MHz wide) allows this targeted blanking.

The technique intervenes at the same location as the temporal blanker, which is after the ADC. The incoming samples are successively processed by groups of N samples (N being fixed). Each group is analyzed in the frequency domain through a Fast Fourier Transform (FFT). The amplitude of each point of this frequency representation is then compared against a certain pre-defined threshold. Note that since the incoming signal is, without interference, dominated by thermal noise, the FFT representation of the incoming signal should ideally be flat (white). This assumption allows the determination of a threshold that would represent the usual noise level, with a certain false alarm rate. Consequently, the points of the signal frequency representation that exceed the threshold are considered corrupted and set to zero. Finally, the inverse FFT of each manipulated group of the incoming signal is performed and the resulting temporal signals are concatenated so as to obtain the processed signal back in the time domain to feed the acquisition/tracking modules. Figure 4 represents the implementation architecture of the technique while Figure 5 represents the different steps of the interference removal process when a strong DME pulse pair is present.

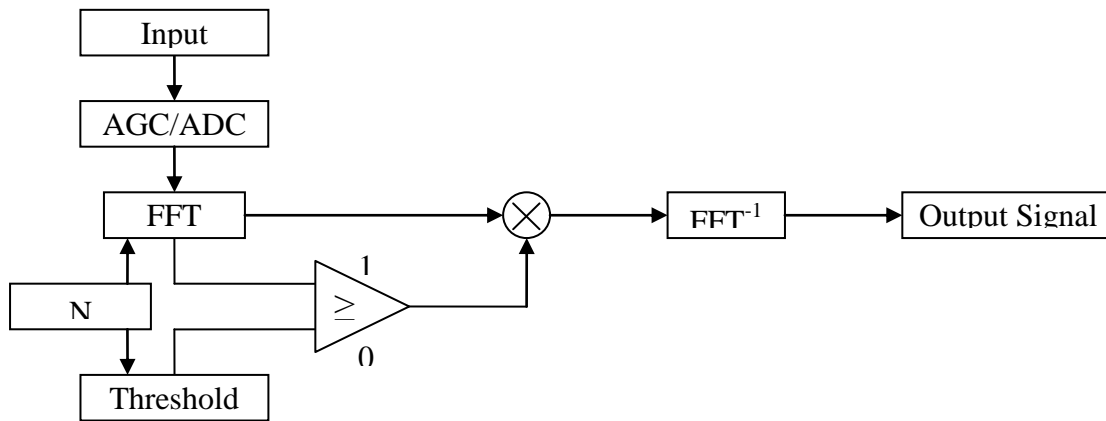


Figure 4 - FDAF Architecture

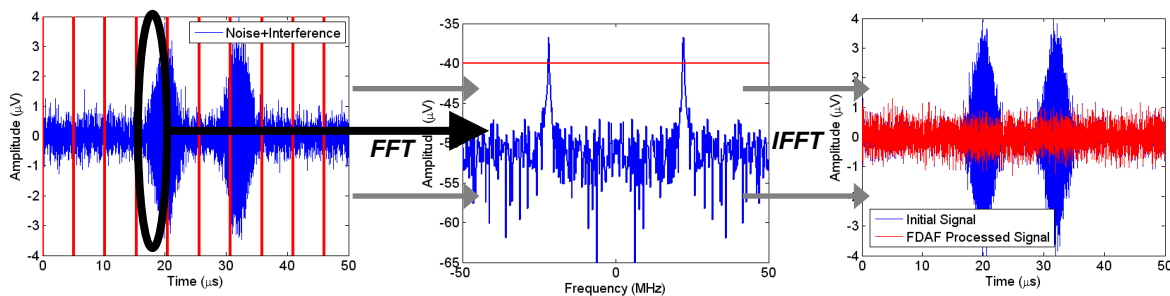


Figure 5 - FDAF Principle Illustration

The FDAF computation load, associated with the two Fourier transforms required, is much more important than the temporal blanker one. It is understood that a large number of samples increase the frequency resolution of the Fourier transform and would likely result into a more relevant blanking technique. However, it will also induce a dramatical increase in the computation load. A trade-off between performance and computation load has then to be found and due to the high sampling frequency required due to the wide E5a and E5b bands, the actual value of N should be chosen fairly low.

The estimated C/N_0 degradations due to DME/TACAN and JTIDS/MIDS (case VIII) pulsed interference are summarized in **Table 2**. The simulations were conducted above the European hot spot. Two different configurations of FDAF were tested: the use of $N=64$ and $N=128$ with a sampling frequency of 100 MHz, as the degradation depends on the number of samples used in the FFT estimation.

C/N ₀ degradation (dB) @ FL 400	Europe
	<i>Galileo E5a</i>
Temporal Blanker	10 dB
FDAF 128 (1920 operations)	4 dB
FDAF 64 (832 operations)	6.62 dB

Table 2 - Simulation Results

These simulation results are presented in [Raimondi]. Table 2 shows the performance improvement when doubling the window size, which was expected for the following reasons:

- Because of the considered sampling frequency (100 MHz), only a small part of one DME/TACAN pulse is included in the 64 or 128 samples used in the FFT computation. It means that increasing the window size increases the amount of pulse observed, and so the amount of power represented by the Fourier transform. A higher peak is then observed,
- The Fourier Transform is defined with a thinner resolution, the same frequency range ($[-F_s/2, F_s/2]$) being represented with twice more points. It should result in a more selective filtering inducing less useful signal is removed.

Note the C/N_0 degradation result over the hot-spot for the temporal blanker is different from the figure in Table 1 (degradation of 8.9 dB). This is due to different simulation assumptions on the RF/IF filters, blanking threshold etc... However, for the sake of comparison between performance of the temporal blanker and FDAF, figures of Table 2 are relevant. The improvement brought by the frequency-domain blanker is clear from Table 2. The C/N_0 degradation is significantly decreased. This means, from an aviation point of view, that if FDAF is used instead of temporal blanker, the signal processing complexity would be reduced. The resulting increase of post-correlation C/N_0 can be exploited in different ways. For instance, the margin with respect to interference-induced effects is increased. Another example is that the number of required correlators to meet the EUROCAE acquisition specifications can be decreased. Of course, this has to be counterbalanced with the increased receiver complexity.

3.3 Acquisition Process

The acquisition process consists of a two-dimensional search both in time and in frequency. Indeed, because the user and satellite positions are initially not known, or known with an uncertainty, the received code phase must be searched. Also, relative changes in time in user/satellite distances create a Doppler frequency that needs to be searched as well. Moreover uncertainty on receiver clock time must be accounted for.

3.3.1 Temporal Acquisition

A previous paper [Bastide2] has demonstrated the improvement brought by the combination of both data and pilot correlator output samples in the case of QPSK signals (i.e. GPS L5). The improvement pertains to the probability of signal detection and the mean acquisition time as well. This combined (data plus pilot) processing allows an improvement of about 2 dB on the required C/N_0 given the mean acquisition time. For this analysis, Galileo E5a and E5b signals were considered as two separate QPSK signals. So as to search a single code/frequency bin for either E5a or E5b, four elementary hardware correlators are required: two for each component (data and pilot) and two for each channel (I and Q). The considered acquisition process structure is depicted in Figure 6.

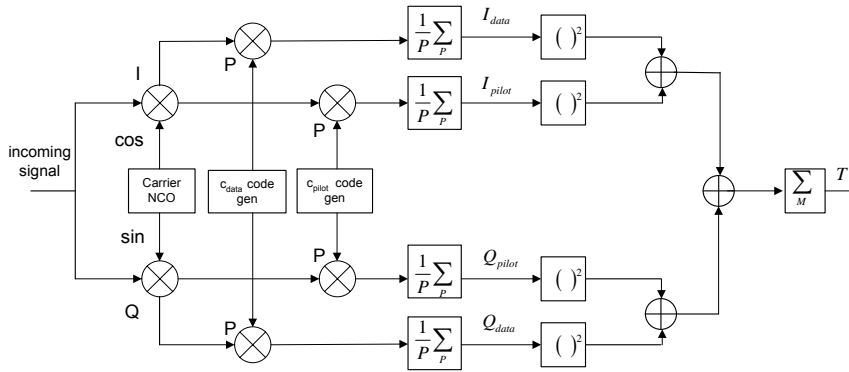


Figure 6

Figure 6 - Acquisition Process Structure

where

- P is the number of cumulated samples so that the coherent integration time T_p equates $P.T_s$ with T_s the sampling period. The predetection bandwidth is $f_p=1/T_p$
- I_{data} , Q_{data} , I_{pilot} and Q_{pilot} are respectively the inphase/quadrature correlator output samples of the data and pilot components
- M is the number of non-coherent integrations

The acquisition process is then based on a test statistic: either the signal is present in the code/Doppler bin or it is not. The decision test T is simply expressed as

$$T = \sum_M (I_{data}^2 + Q_{data}^2 + I_{pilot}^2 + Q_{pilot}^2)$$

This decision test follows a centred chi-square distribution with $4M$ degrees of freedom in presence of noise, and a non-central chi-square distribution with $4M$ degrees of freedom in presence of the useful signal. More information on the statistics of the test are provided in [Bastide2].

The RTCA MOPS DO 229 [RTCA DO-229] specified the initial acquisition requirement as follows. The equipment shall be capable of acquiring satellites and determining a position without any initialization information, including time, position, and GPS and WAAS almanac data. In addition, with latitude and longitude initialized within 60 nautical miles, with time and date within 1 minute, with valid almanac data and unobstructed satellite visibility, and under interference conditions detailed in Appendix C of reference [RTCA DO-229] and under the minimum signal conditions defined in Section 2.1.1.10 of reference [RTCA DO-229], the time from application of power to the first valid position fix shall be less than 5 minutes. This requirement is applicable for an aircraft on the ground and also in flight after a power outage. The receiver is said to be in “warm start”. Note EUROCAE WG62 adopted the same requirement for future Galileo receivers. It has been shown in [GalMOPS] that this requirement can be satisfied provided the C/N_0 is in the range 29-31 dB/Hz and the hardware complexity is, respectively, of 2500 to 300 hardware correlators.

3.3.2 Frequency-domain Acquisition

Over the past few years, both Digital Signal Processors (DSP) and microprocessors (μP) have experienced a tremendous increase of their computing power. The software-based approach takes advantage of the capacity of the DSPs and μP s to handle specific mathematic functions such as the Discrete Fourier Transform (DFT). The digital autocorrelation function R_c of a spreading code c of period N can be written as

$$R_c(m) = \frac{1}{N} DFT^{-1} [DFT[c(n)] \cdot \overline{DFT[c(n)]}]$$

Figure 7 illustrates the typical correlator architecture as implemented in a software-based receiver. The local replica of the spreading code is first Fourier-transformed and conjugated. The incoming signal is also Fourier transformed and both quantities are then multiplied. The inverse Fourier transform is computed to finally obtain the output of the correlator.

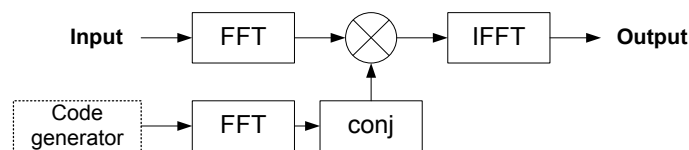


Figure 7 - FFT-based Correlator of a Software-Based GNSS Receiver.

The design of such a correlator has also the advantage of being well suited to process analytic signals so that both the inphase (real part) and quadrature (imaginary part) channels can be processed together [Kubrak]. Moreover, such architecture makes it possible to process at once n ms of signal. In other words, all possible code phase bins are explored at once for a given Doppler shift, which tremendously decreases the acquisition processing time, as it will be shown in the following. One particularity of the software-based acquisition is that the time needed to successfully acquire one GNSS signal is composed of two parts. The first one is the useful signal duration which has the similar meaning as in the temporal acquisition technique case. The second one is the time needed by the DSP or the μP to compute the FFTs on the useful signal. The time is very dependent on the computing capacities of the DSP or μP used. This specific time can not be neglected. The acquisition procedure is speed up since all the code phase bins can be explored at once. Opposite, processing time is added to the overall time needed to successfully acquire one GNSS signal.

In a software-based acquisition, the resolution of the code phase bins depends on the sampling frequency of the digitized signal. Usually, the main lobe of the signal spectrum is used for further processing, meaning that the sampling rate is at least twice those of the code. As a consequence, the code phase bin resolution is at least equal to half a chip, which is consistent with the current state of the art processing. A better code phase bin resolution can also easily be achieved using a higher sampling rate. The performance of the temporal acquisition technique and the frequency-based one were compared and assessed through Monte-Carlo simulations on a typical case. Equivalent acquisition strategies were chosen and the different simulation characteristics are listed below:

- The simulations are done for a false alarm probability P_{fa} of 10^{-4} .
- Dwell time of 100 ms (1 ms coherent integration and 100 non-coherent integrations)
- Three typical probabilities of detection were analysed, namely 0.9, 0.8 and 0.6. The corresponding C/N_0 values equate 32.7 dBHz, 32.3 dBHz and 31.7 dBHz. (see [Bastide1])
- The receiver is assumed to be in the warm start conditions described in section 3.3.1 which correspond to RTCA and EUROCAE assumptions. These conditions imply a Doppler uncertainty of ± 1 kHz (4 bins for a search step of 500 Hz) and a full code phase uncertainty so that all code bins have to be explored ($2 \cdot 10230$ code bins for a search step of half a chip).
- In the case of the frequency-domain acquisition, for each Doppler bin every peak above a determined threshold is tested as the potential true correlation peak. A penalty factor of 1s is added to the overall successful acquisition time in case of false alarm. An equivalent strategy is adopted for the time-domain acquisition process. Code/Doppler bins are swept until the test statistic is above the acquisition threshold, then a penalty factor of 1 s is added in case of false alarm. The single-dwell time strategy was simulated [Holmes].

The Cumulative Density Functions of the acquisition time for both strategies are in Figure 8.

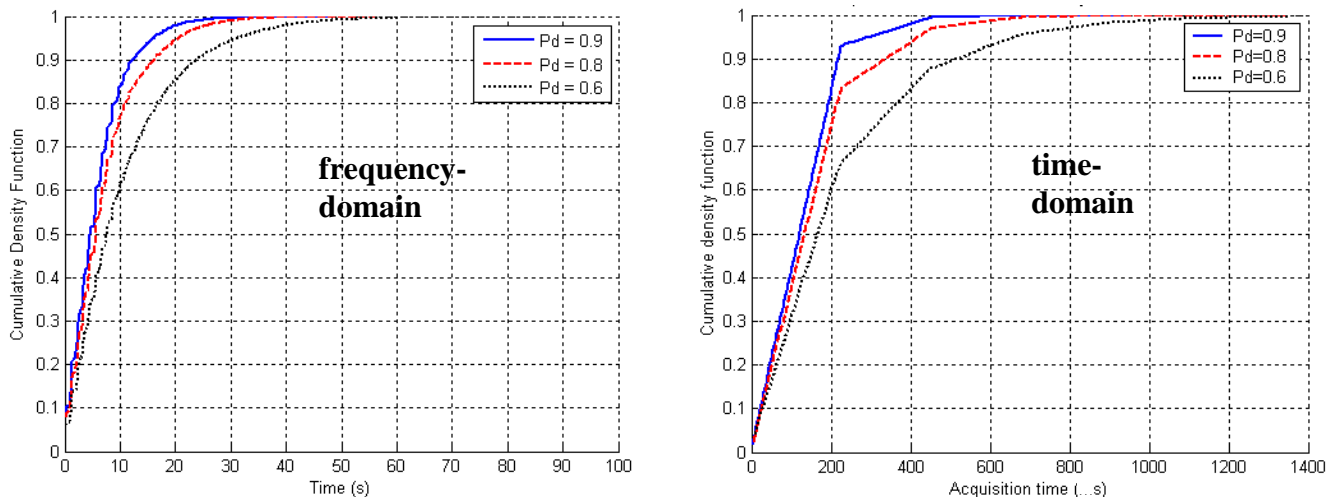


Figure 8 – Acquisition Time Cumulative Density Functions for $P_d = 0.9, 0.8$ and 0.6 .

These density functions clearly show the tremendous improvement brought by the FFT-based correlators with respect to acquisition time as compared to the classic temporal acquisition case. For instance, assuming a probability of detection of 0.9, the acquisition time is lower than about 12 s with a probability of 0.9 with the FFT-based method while the equivalent value is about 200 s for the time-domain strategy.

3.4 Tracking Process

The interim Galileo MOPS [GalMOPS] requires civil aviation receivers to track independently Galileo E5a and E5b signals. A coherent tracking of the wideband Galileo E5 signal is possible but has not been considered yet by civil aviation because of the increased interference risk as well as the associated integrity risk. Galileo E5a and E5b are processed as two individual QPSK signals. Thanks to the presence of pilot components, it is possible to use a pure Phase Lock Loop (PLL) whose integration time is no longer limited by data bits transitions. In this case, the tracking process is more robust (i.e. lower tracking threshold). However, the increased oscillator noise within the tracking loop because of longer integration times has to be considered with attention (see [Hegarty2] on this subject).

The nominal case corresponds to the dual-frequency mode where the receiver can compute a iono-free pseudo-range measurement according to the following equation:

$$PR = \frac{PR(f2) - \gamma PR(f1)}{1 - \gamma}$$

where,

- PR is the pseudo-range corrected from ionospheric delay
- $PR(f)$ is the pseudo-range measured on the frequency f
- $\gamma = (f1/f2)^2$

EUROCAE WG62 computed the User Equivalent Range Error (UERE) for mono-frequency and dual-frequency Galileo users. This UERE is the one-sigma value of the pseudo-range error. It accounts for effects of clock/ephemeris errors, the receiver noise, multipaths, troposphere and residual ionospheric delay correction in the single-frequency mode. The obtained figures are:

- mono-frequency mode: 12 m
- dual-frequency mode: 2 m

3.5 Interference Detection Techniques

So as to declare a frequency is lost, the receiver must decide whether the navigation signals transmitted on that frequency by SVs still provide the required levels of performance and so should still be used to perform, for instance, dual-frequency measurements. Strong interference is the main reason for a receiver to loose a frequency since it impacts, unlike multipath, all the signals transmitted on the considered band by the different constellations. Different methods are proposed to detect in-band interference and are presented below.

3.5.1 Computation of the C/N_0

Signal quality may be assessed by the SNR estimate, computed from Inphase and Quadrature samples, at correlator output. This quantity is degraded by imperfect code and carrier tracking and may be directly related to the BER (see the sections on tracking and data demodulation thresholds computation). In general, a receiver declares a signal is present or lost if its estimated SNR is respectively above or below a threshold for a period of time. This threshold is set so that it corresponds to given tracking and demodulation performance (i.e. 27 dBHz for GPS L5). So if all, or a majority of, the signals transmitted on the same frequency have SNRs below the threshold then it is likely a harmful interferer is present in the band. The more there are estimates below the given threshold, the more likely an interference is present.

Such a test on the estimated C/N_0 may be combined with a detection algorithm so as to ensure an in-band interferer is really present. Two of them are proposed in the following.

3.5.2 Chi-square Test at the ADC Level

ADC with supplementary bins may be used to better represent the thermal noise Gaussian distribution through increased resolution. This additional resolution could bring higher interference detection performance. Recall that the ADC bins distribution, a Gaussian, is maintained constant, in the absence of any perturbation, as a result of the AGC gain adaptation. If an interference source is introduced, AGC gain decreases in order to maintain the Gaussian shape. Thus, even in presence of interference, the ADC distribution may seem to be nominal. However if the resolution is increased, the ADC distribution may clearly represent the distribution of the incoming signal. This distribution was previously hidden because of the low resolution. Indeed, the incoming signal distribution shape is unchanged by the AGC that only applies a gain. Thus it is possible to implement a test on ADC bins distribution changes to detect interference. A straightforward approach is to use the Chi-Square test to decide if two sets of data are consistent. This method has been introduced in [Bastide3].

3.5.3 Use of Multicorrelator Receivers

The impact of a single CW interference on the correlator output has been characterized in [Macabiau; Bastide4]. It has been shown that it adds to the PRN correlation function a sine wave whose main parameters are:

- An amplitude dependent upon the CW power, the amplitude of the closest PRN spectral line compared to the CW frequency, and the integration time, and
 - A frequency equal to the relative incoming CW frequency with respect to the useful signal central frequency
- Thus, using these properties, the observation of the correlation function can be used to detect the presence of a CW.

A multicorrelator receiver has the ability to use several correlators with different offsets from the prompt correlator. Thus it allows visualizing, with a certain resolution and over a certain span, the correlation function (this being true for the In-phase and Quadra-phase correlation values used by the receiver). An example of the multicorrelator output is shown in Figure 9. The presence of a sine function, due to a high CW can be easily identified. In this figure, the period of this sine function is 4.5 chips, which corresponds to a frequency of 227 kHz. Many similar tests were carried out and validated the theoretical derivation.

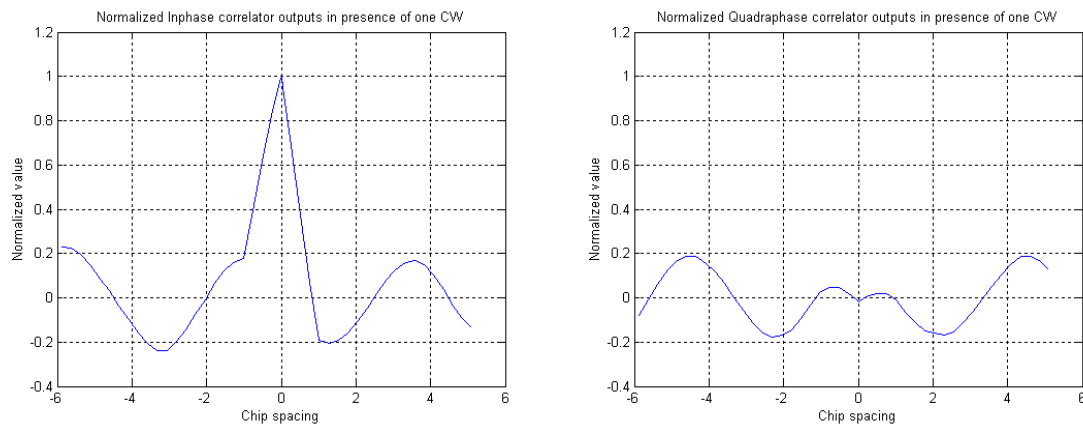


Figure 9 - Observed Inphase and Quadraphase correlator outputs when a CW hits a PRN code spectrum line

The methodology to detect and characterize the CW is detailed in [Bastide4]. First, the multiple correlators output have to be normalized in order to have the prompt correlator with a unit magnitude. In that way, it unifies the following characterization tool. This normalization can be done, for instance, through an assessment of the incoming signal power. Since the shape of the normalized PRN autocorrelation function is known, it is then possible to subtract it from the correlator outputs in order to have only the CW-induced sine-wave present.

The residuals of the correlators' output are then analyzed in the frequency domain in order to detect a peak that would indicate the presence of a sine function. The detection threshold can be, as an example, determined taking into account given Pfa and Pmd values as well as the incoming noise power that could be estimated through a preliminary training period.

Once a CW interference is detected, a specialized procedure is run using the residuals of the correlators' output to determine the number of sine functions present and their respective amplitude, phase, and frequency. This process uses parametric methods based on Auto-regressive models such as Prony or ESPRIT. It is obvious that the estimation process will be dependent upon the correlators location, and the CW power. The correlator spacing should be chosen according to the maximum expected frequency of the feared CW (within 1 MHz for the GPS C/A and 10 MHz for GPS L5 or Galileo E5a or E5b for instance). Also, it has to be emphasized that a high CW power would be more accurately characterized.

Conclusions

This paper gives an overview of the main signal processing techniques which have been considered for civil aviation receivers. These techniques concern signal RF/IF filtering, signal acquisition, signal blanking, signal tracking and interference detection. While the typical techniques considered so far by civil aviation were highlighted, new and more efficient methods were presented as well. For signal acquisition and blanking, they work in the frequency domain. The achieved performance improvements were indicated but they have to be balanced against the increased complexity. One may guess that in the future, technological progresses will allow such techniques to be implemented in civil aviation receivers.

References

- [GalICD] *Galileo Open Service Signal In Space Interface Control Document (OS SIS ICD) Draft 0*, the European Space Agency/Galileo Joint Undertaking, May 2006
- [Rebeyrol et al., 2005] *BOC Power Spectrum Densities*, E. Rebeyrol, C. Macabiau, L. Lestarquit, L. Ries, J-L. Issler, M-L. Boucheret, M. Bousquet – Proceedings of The Institute of Navigation NTM Meeting, San Diego, CA, January 2005.
- [GalMOPS] *Interim Minimum Operational Performance Specification for Galileo Satellite Positioning Receiver*, EUROCAE, May 2006
- [RTCA DO-292] *Assessment of Radio Frequency Interference Relevant to GNSS L5/E5a frequency Bands DO-292*, RTCA, July 2004
- [Grabowsy] *Characterization of L5 Receiver Performance Using Digital Pulse Blanking*, Grabowski, J, Hegarty, C, Proceedings of The Institute of Navigation GPS Meeting, Portland, OR, September 2002
- [Hegarty] *Methodology for Determining Compatibility of GPS L5 with Existing Systems and Preliminary Results*, Hegarty, C., T. Kim, S. Ericson, P. Reddan, T. Morrissey, and A.J. Van Dierendonck,, Proceedings of the Institute of Navigation Annual Meeting, Cambridge, MA, June 1999
- [Tran] *Performance Evaluations of the New GPS L5 and L2 Civil (L2C) Signals*, M.Tran, C.Hegarty, Proceedings of The Institute of Navigation NTM Meeting, Anaheim, CA, 2003
- [Bastide1] *Analysis of the feasibility and Interests of Galileo E5a/E5b and GPS L5 for Use with Civil Aviation*, PhD dissertation, October 2004.
- [Bastide2] *Analysis of L5/E5 Acquisition, Tracking and Data Demodulation Thresholds*, F. Bastide, O. Julien, C. Macabiau, B. Roturier, Proceedings of the Institute of Navigation GNSS Meeting, Portland, OR, September 2002
- [Bastide3] *Automatic Gain Control (AGC) as an interference assessment tool*, F. Bastide, D. Akos, C. Macabiau, B. Roturier, Proceedings of the Institute of Navigation GNSS Meeting, Portland, OR, September 2003
- [Bastide4] *GPS Interference Detection and GPS Interference Detection and Identification Using Multicorrelator Receivers*, F. Bastide, E. Chatre, C. Macabiau, Proceedings of The Institute of Navigation GPS Meeting, Salt Lake City, UT, September 2001
- [Raimondi] *Performance Assessment and Implementation Constraints Analysis of Frequency Domain Adaptive Filtering for Pulsed Interference Mitigation in GNSS Receivers*, Proceeding of the Institute of Navigation GNSS Meeting, Fort Worth, Sept. 2006
- [RTCA DO-229] *Minimum Operational Performance Standards for Global Positioning System/Wide Area Augmentation System Airborne Equipment* , RTCA SC-159
- [Kubrak] *Analysis of a software-based A-GPS acquisition performance using statistical processes*, D. Kubrak, C. Macabiau, M. Monnerat, Proceedings of The Institute of Navigation NTM Meeting, San Diego, CA, January 2005.
- [Holmes] *Coherent Spread Spectrum Systems*, J.K Holmes, New York, John Wiley & Sons, 1982
- [Macabiau] *Use of Multicorrelator Techniques for Interference Detection*, C. Macabiau, O. Julien and E. Chatre, Proceedings of The Institute of Navigation NTM Meeting, Long Beach, CA, Jan 2001